Indian J. Pure Appl. Math., **45**(4): 415-432, August 2014
© Indian National Science Academy

ANALYTICAL AND NUMERICAL SIMULATION INVESTIGATION IN EFFECTS OF RADIATION AND POROSITY ON A NON-ORTHOGONAL STAGNATION-POINT FLOW TOWARDS A STRETCHING SHEET

D. D. Ganji*, S. Jafarmadar**, B. Jalilpour**, R. Rahimi**, A. B. Shotorban*** and Seyed H. Hashemi Kachapi*

**Department of Mechanical Engineering, Babol Noshirvani University of Technology, Babol, Iran*

***Department of Mechanical Engineering, Faculty of Engineering, Urmia University, Urmia, Iran*

****Department of Mechanical Engineering, Islamic Azad University, Sari Branch, Sari, Iran*

e-mail: ddg_davood@yahoo.com

(*Received* 5 *May* 2013; *after final revision* 7 *July* 2013; *accepted* 8 *July* 2013)

The steady two-dimensional non-orthogonal flow near the stagnation point on a stretching sheet embedded in a porous medium in the presence of radiation effects is studied. Using similarity variables, the nonlinear boundary-layer equations are solved analytically by homotopy perturbation method (HPM) employing Padé technique. Comparison between the results of HPM-Padé solution and numerical simulation as well as some other results which are available in the literature, demonstrates a very good agreement between them and the HPM-Padé solution provides a convenient way to control and adjust the convergence region of a system of nonlinear boundary-layer problems with high accurate. The effect of involved parameters such as striking angle, radiation parameter, porosity parameter and the Prandtl number on flow and heat transfer characteristics have been discussed with more details.

Key words : Nonlinear boundary-layer problem; HPM-Padé; stagnation point; non-orthogonal flow; stretching sheet; heat transfer.

1. INTRODUCTION

Stagnation point flow is observed in almost all types of the flow when fluid become in contact with a solid boundary and forms a boundary layer. In the vicinity of the stagnation point fluid velocity reduces to zero and flow reaches its maximum pressure at the stagnation point. Due to numerous industrial applications, boundary layer flow past a stretching plate has attracted considerable attention of researchers in the recent years. Such applications include polymer processing, metal working, extrusion of a polymer, hot rolling, wire drawing, glass fiber, paper production, drawing of paper films, etc. [1].

Hiemenzwas [2] pioneer in using similarity transformation to reduce governing equations of two-dimensional stagnation point flow on a stretching sheet to ordinary differential equations. Later, Chiam [3] carried a study on stagnation point flow from different point of views such as oblique or normal flow or axisymmeteric flow. Moreover, heat transfer in stagnation point flow was subject of interest for many recent studies [4-10]. In some other investigations, Magneto Hydro Dynamic (MHD) flow adjacent to the stagnation point was studied both numerically and analytically [11-15]. Along with the other authors, McLeod *et al.* have proved the uniqueness of the solution of the Navier-Stokes equation in the stretching sheet case [16]. A fundamental study on the characteristics of the boundary layer in stretching sheets is carried by Mahapatra *et al.* [4]. It is shown that a boundary layer is formed near the stretching surface and that the structure of this boundary layer depends on the ratio of the velocity of the stretching surface to that of the frictionless potential flow in the neighborhood of the stagnation point.

Nonlinear partial differential equations (NPDE), arising in the vast diversity of engineering and scientific problems, possess a vital role in many scientific problems. Although, there exist some analytical solutions for a limited number of partial differential equations, however, they are not applicable to real world situation. In the recent decades, many efforts are dedicated devising new methods for solution of nonlinear partial equations. These methods include numerical and semi-exact methods. Although numerical methods are gaining more and more popularity in the scientific community, they have some limitations and issues such as convergence and stability. Perturbation method is a semi-exact method which requires finding a small parameter and inserting it into the equation. Although this method is can easily implement in symbolic computations softwares, difficulties in finding the small parameter are the deficiency of this method. Beyond, no all nonlinear partial equations have some small/large perturba-

tion parameters. Recently, Liao has proposed a method which doesn't involve any small/large perturbation parameters called homotopy analysis method (HAM) [17, 18]. This semi-exact method is very flexible one especially in adjustability of the convergence area by mean of an auxiliary parameter. However, it necessities developing a rather complex programming code. Another method embracing both advantaged of these methods is suggested by He [19-21]. He's Homotopy Perturbation Method (HPM) combines ease of implementation of the perturbation methods with the flexibility of the Homotopy Analysis Method. It still doesn't consist any small/large perturbation parameters in the solution procedure. Recently, the homotopy perturbation method has been used to solve a wide range of problems [22-26].

The present paper aims to study two dimensional steady non-orthogonal flow near the stagnation point on a stretching sheet embedded in a porous medium in the presence of radiation effects is obtained by combining homotopy perturbation method and Padé approximation. To the best of our knowledge, there are only a few papers in the literature dealing with oblique stagnation point flow problem, but none of them have applied HPM– Padé solution to obtain a semi exact solution for this problem [27, 28]. The HPM-Padé technique has been successfully implemented to solve them by converting the series solutions into the diagonal Padé techniques.

2. Analysis of the Homotopy Perturbation Method

To illustrate the basic idea of this method [19, 20], we consider the following nonlinear differential equation:

$$A(u) - f(r) = 0, \qquad r \in \Omega \tag{1}$$

Considering the boundary conditions of:

$$B\left(u, \frac{\partial u}{\partial n}\right) = 0, \qquad r \in \Gamma \tag{2}$$

Where A is a general differential operator, B a boundary operator,$f(r)$ a known analytical function and Γ is the boundary of the domain Ω. The operator A can be divided into two parts of L and N, where L is the linear part, while N is a nonlinear one Eq. (1) therefore can be rewritten as follows:

$$L(u) + N(u) - f(r) = 0, \qquad r \in \Omega. \tag{3}$$

The homotopy perturbation structure is shown as follows:

$$H(\nu, p) = (1-p)[L(\nu) - L(u_0)] + p[A(\nu) - f(r)] = 0 \tag{4}$$

where:

$$\nu\,(r,p) : \Omega \times [0,1] \rightarrow R. \tag{5}$$

We can assume that the solution of Eq. (5) can be written as a power series in p, as follows:

$$\nu = \nu_0 + \varepsilon\nu_1 + \varepsilon^2\nu_2 + \ldots \tag{6}$$

Setting p = 1 result in the approximate solution is:

$$V = \lim_{p\rightarrow 1} \nu = \nu_0 + \nu_1 + \nu_2 + \ldots \tag{7}$$

Combination of the perturbation method and the homotopy method is called HPM, which lacks the limitations of the traditional perturbation methods, although this technique has full advantages of the traditional perturbation techniques.

3. Problem Formulation

A schematic view of an incompressible fluid near a non-orthogonal stagnation point on a stretching sheet is depicted in Fig. 1. Fluid is considered in the porous medium obeying Darcy law in the presence of radiation effect. The stretching sheet has uniform temperature T_w and linear velocity u_w This figure shows two dimensional stagnation point flow over a surface stretching in the direction of the x axis. y axis is a supposed to be normal to the stretching wall. The wall velocity assumed to be zero at the stagnation point and increases linearly with x. The flow domain is constrained to y>0.

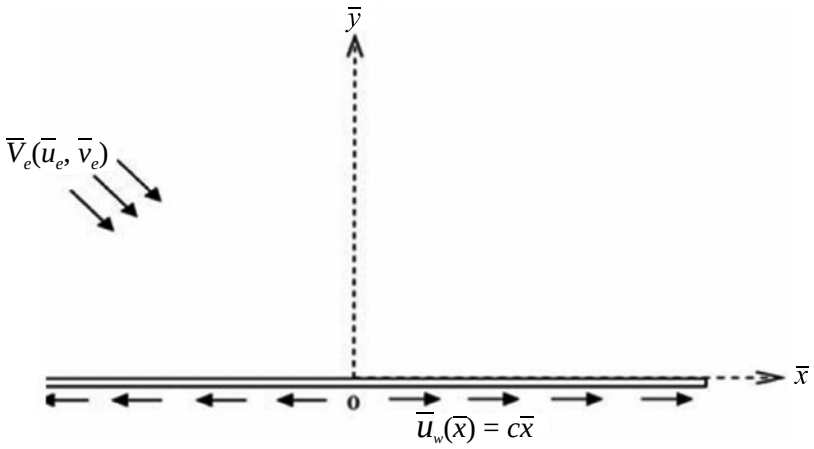

Fig.1. Physical model

It is assumed that. The governing equations of mass, momentum and energy underlying above assumptions with neglecting external field are given by:

$$\frac{\partial u}{\partial x}+\frac{\partial v}{\partial y}=0 \tag{8}$$

$$u\frac{\partial u}{\partial x}+v\frac{\partial u}{\partial \bar{y}}=-\frac{1}{\rho}\frac{\partial p}{\partial x}+\nu\nabla^2 u-\frac{u\nu}{k} \tag{9}$$

$$u\frac{\partial v}{\partial x}+v\frac{\partial v}{\partial y}=-\frac{1}{\rho}\frac{\partial p}{\partial y}+\nu\nabla^2 v-\frac{u\nu}{k} \tag{10}$$

$$\rho c_p\left(u\frac{\partial T}{\partial x}+v\frac{\partial T}{\partial y}\right)=K\frac{\partial^2 p}{\partial y^2}-\frac{\partial q_r}{\partial y}. \tag{11}$$

Where *u* and ν are the velocity component in the *x* and *y* directions, *p* is the pressure fluid, υ is kinematic viscosity, *k* is permeability of saturated porous medium, *T* is the temperature, ρ is density of the fluid, *K* is thermal conductivity and c_p is specific heat at constant pressure. We assume that the boundary conditions of Eqs. (8)-(11) are

$$u=u_w(x)=cx,\quad \nu=0,\quad T=T_w\quad at\quad y=0,$$

$$u=axsin\gamma+bycos\gamma,\quad \nu=-aysin\gamma,\quad T=T_\infty\quad as\quad y\to\infty. \tag{12}$$

Where a, b and c are positive constants with the dimension of (time)$^{-1}$ indicating potential flow and linear shear flow parallel to the stream wise direction (shear stress b) contributions into the oblique flow respectively. Using this set of similarities from [27]:

$$\xi=(c/\upsilon)^{0.5}x,\quad \eta=(c/\upsilon)^{0.5}y,\quad \psi(\xi,\eta) \tag{13}$$

and taking into account the definition of the stream function near the stretching wall as:

$$\psi=\xi f(\eta)+g(\eta) \tag{14}$$

The Navier–Stokes equation reduces to:

$$f'''(\eta)+ff''-f'^2-A(f'-\lambda sin\gamma)+\lambda^2 sin^2\gamma=0 \tag{15}$$

$$g'''(\eta)+fg''-f\,'g'-A(g\,'-r\eta cos\gamma)-\alpha r cos\gamma=0 \tag{16}$$

Where λ = a/c and r = b/c are positive constants. The boundary conditions are defined as:

$$f(0) = 0, f'(0) = 1, f\,'(\infty) = \lambda \sin\gamma, \qquad g(0) = 0, g'(0) = 0, g''(\infty) = r\cos\gamma. \quad (17)$$

Also

$$f(\infty) = \lambda\eta \sin\gamma + \alpha, \qquad g(\infty) = r\eta\cos\gamma. \quad (18)$$

And can be obtained, where α is a real constant and could be obtained by solving Eq. (15). By using

$$g(\eta) = rh(\eta)\cos\gamma \quad (19)$$

Eq. (16) reduces to:

$$h''' + fh'' - f'h' - A(h'-\eta) - \alpha = 0 \quad (20)$$

$$h(0) = 0 h'(0) = 0, h''(\infty) = 1. \quad (21)$$

Radiative heat flux q_r in governing boundary layer equation of energy (11) is approximated by Rosseland approximation, which gives $q_r = -\dfrac{4\sigma}{3k_1}\dfrac{\partial T^4}{\partial y}$, where σ and k_1 are Stefan-Boltzmann constant and absorption coefficient, respectively. It is assumed that the temperature difference within the flow is so small and T^4 can be expressed as a linear function of T. This can be obtained by expanding T^4 in a Taylor series about T and neglecting the higher order terms. Thus we get, $T^4 \cong 4T_\infty^3 T - 3T_\infty^4$. Heat is transferred by forced convection which involve the only normal component of flow field, therefore θ (η) is dimensionless temperature defined as:

$$\theta(\eta) = \frac{T - T_\infty}{T_w - T_\infty} \quad (22)$$

Using this in energy Eq. (11), we have

$$\theta''\left(1 + \frac{4R}{3}\right) + \Pr .f.\theta = 0 \quad (23)$$

With the following boundary conditions:

$$\theta(0) = 1, \quad \theta(\infty) = 0 \quad (24)$$

The non-dimensional stream function ψ now reads:

$$\psi(\xi, \eta) = \xi f(\eta) + rcos\gamma h(\eta). \quad (25)$$

The skin friction is given in non-dimensional form by:

$$\tau_w = \left(\frac{\partial^2 \psi}{\partial y^2}\right)_{y=0} = \xi f''(0) + r\cos\gamma h''(0) \tag{26}$$

The dividing streamlines ψ=0 and the curve *u*=0 intersect the wall at the stagnation point where τ_w=0. Hence, the location of the stagnation point ξ_s is given by

$$\xi_s = \frac{-r\cos\gamma h''(0)}{f''(0)}. \tag{27}$$

4. Homotopy Perturbation Solution

In this section, we will apply HPM to nonlinear ordinary differential equation Eqs. (15), (16) and (23). According to HPM, we can construct a homotopy of Eqs. (15), (16) and (23) as:

$$H(f,p) = (1-p)(f''' - f_0''') + p(f''' + ff'' - f'^2 - A(f' - \lambda\sin\gamma) + \lambda^2\sin(\gamma)^2) = 0 \tag{28a}$$

$$H(h,p) = (1-p)(h''' - h_0''') + p(h''' + fh'' - f'h' - \alpha - A(h' - \eta)) = 0 \tag{28b}$$

$$H(\theta,p) = (1-p)(\theta''(1+\frac{4R}{3}) - \theta_0'') + p(\theta''(1+\frac{4R}{3}) + \Pr.f.\theta) = 0 \tag{28c}$$

We consider

$$f(\eta) = f_0(\eta) + pf_1(\eta) + p^2 f_2(\eta) + p^3 f_3(\eta) + \ldots \tag{29a}$$

$$h(\eta) = h_0(\eta) + ph_1(\eta) + p^2 h_2(\eta) + p^3 h_3(\eta) + \ldots \tag{29b}$$

$$\theta(\eta) = \theta_0(\eta) + p\theta_1(\eta) + p^2\eta_2(\eta) + p^3\theta_3(\eta) + \ldots \tag{29c}$$

Substituting *f, h* and θ Eqs. 28(a,b,c) into Eqs. 29(a,b,c) and some simplification and rearranging based on powers of p-terms, we have:

$$p^0: \quad f_0''' = 0, \quad h_0''' = 0, \quad \theta_0'' = 0 \tag{30}$$

and boundary conditions are:

$$\begin{aligned} &f_0(0) = 0, && f'_0(0) = 1, && f_0''(0) = \alpha_1 \\ &h_0(0) = 0, && h_0'(0) = 1, && h_0''(0) = \alpha_2 \\ &\theta_0(0) = 1, && \theta_0'(0) = \alpha_3 \end{aligned} \tag{31}$$

$$
\begin{aligned}
&p^1: \\
&f_1'''(\eta) + f_0 f_0'' - f_0'^2 - A f_0' + A\lambda sin\gamma + \lambda^2 sin^2\gamma = 0 \\
&h_1''' + f_0\, h_0'' - f_0'\, h_0' - A h_0' + A\eta - \alpha = 0 \\
&\theta_1'' + \frac{4R}{3}\theta_1'' + \Pr . f_0 . \theta_0' = 0
\end{aligned} \tag{32}
$$

and boundary conditions are:

$$
\begin{aligned}
&f_1(0) = 0, \qquad f'_1(0) = 1, \qquad f_1''(0) = 0 \\
&h_1(0) = 0, \qquad h_1'(0) = 1, \qquad h_1''(0) = 0 \\
&\theta_1(0) = 1, \qquad \theta_1'(0) = 0
\end{aligned} \tag{33}
$$

$$
\begin{aligned}
&p^2: \\
&f_2'''(\eta) + f_1 f_0'' - 2 f_0' f_1' - A f_1' + f_0 f_1'' = 0 \\
&h_2''' + f_0\, h_1'' - f_1' h_0' - A h_1' + f_1 h_0'' - f_0' h_1' = 0 \\
&\theta_2'' + \frac{4R}{3}\theta_2'' + \Pr . f_0 . \theta_1' + \Pr . f_1 . \theta_0' = 0
\end{aligned} \tag{34}
$$

and boundary conditions are:

$$
\begin{aligned}
&f_2(0) = 0, \qquad f'_2(0) = 0, \qquad f_2''(0) = 0 \\
&h_2(0) = 0, \qquad h'_2(0) = 0, \qquad h_2''(0) = 0 \\
&\theta_2(0) = 0, \qquad \theta_2'(0) = 0
\end{aligned} \tag{35}
$$

Solving Eqs. (30)-(34) with their boundary conditions Eqs.(31) –(35) give following results:

$$f_0(\eta) = \frac{1}{2}\alpha_1 \eta^2 + \eta \tag{36}$$

$$h_0(\eta) = (1/2)\alpha_2 \eta^2 \tag{37}$$

$$\theta_0(\eta) = \alpha_3 \eta + 1 \tag{38}$$

$$f_1(\eta) = \frac{1}{120}\alpha_1^2 \eta^5 + \left(\frac{1}{24}\alpha_1 + \frac{1}{24}\alpha_1 A\right)\eta^4 + \left(-\frac{1}{6}\lambda^2 sin(\gamma)^2 - \frac{1}{6}A\lambda sin(\gamma) + \frac{1}{6}A + \frac{1}{6}\right)\eta^3 \tag{39}$$

$$h_1(\eta) = \frac{1}{120}\alpha_2 \alpha_1 \eta^5 + \left(\frac{1}{24}A\alpha_2 - \frac{1}{24}A\right)\eta^4 + \frac{1}{6}\alpha\eta^3 \tag{40}$$

$$\theta_1(\eta) = -\frac{1}{8}\frac{Pr\alpha_3\alpha_1}{(4R+3)}\eta^4 - \frac{1}{2}\frac{Pr\alpha_3}{4R+3}\eta^3 \tag{41}$$

$$f_2(\eta) = -\frac{1}{40320}\alpha_1^3\eta^8 + \left(-\frac{1}{5040}\alpha_1^2 + \frac{1}{2520}\alpha_1^2 A\right)\eta^7$$
$$+\left(-\frac{1}{360}\alpha_1\lambda^2 sin(\gamma)^2 - \frac{1}{360}\alpha_1 A\lambda sin(\gamma) + \frac{1}{720}\alpha_1 + \frac{1}{720}\alpha_1 A^2 + \frac{1}{360}A\alpha_1\right)\eta^6$$
$$+\left(-\frac{1}{120}A^2\lambda sin(\gamma) + \frac{1}{120}A^2 - \frac{1}{120}A\lambda^2 sin(\gamma)^2 + \frac{1}{120}A\right)\eta^5 \quad (42)$$

$$h_2(\eta) = -\frac{1}{40320}\alpha_2\alpha_1^2\eta^8 + \left(\frac{1}{2520}A\alpha_1 + \frac{1}{2520}A\alpha_2\alpha_1\right)\eta^7$$
$$+\left(\frac{1}{720}A^2\alpha_2 - \frac{1}{360}\alpha_2 A\lambda sin(\gamma) - \frac{1}{360}\alpha_2\lambda^2 sin(\gamma)^2 + \frac{1}{360}\alpha_2 + \frac{1}{360}A - \frac{1}{720}A^2\right)$$
$$\eta^6 + \left(-\frac{1}{120}\alpha + \frac{1}{120}A\alpha\right)\eta^5 \quad (43)$$

$$\theta_2(\eta) = \frac{1}{(4R+3)^2}\left(-\frac{1}{560}Pr\alpha_3\alpha_1^2 - \frac{1}{420}Pr\alpha_3 R\alpha_1^2 + \frac{1}{56}Pr^2\alpha_3\alpha_1^2\right)\eta^7 + \frac{1}{(4R+3)^2}$$
$$\left(-\frac{1}{60}Pr\alpha_3\alpha_1 RA + \frac{1}{8}Pr^2\alpha_3\alpha_1 - \frac{1}{80}Pr\alpha_3\alpha_1 - \frac{1}{60}Pr\alpha_3\alpha_1 R - \frac{1}{80}Pr\alpha_3\alpha_1 A\right)\eta^6$$
$$+\frac{1}{(4R+3)^2}\left(\frac{1}{10}Pr\alpha_3 AR\lambda sin(\gamma) - \frac{3}{40}Pr\alpha_3 - \frac{1}{10}Pr\alpha_3 AR + \frac{3}{40}Pr\alpha_3 A\lambda sin(\gamma)\right.$$
$$\left.-\frac{3}{40}Pr\alpha_3 A + \frac{3}{40}Pr\alpha_3\lambda^2 sin(\gamma)^2 - \frac{1}{10}Pr\alpha_3 R + \frac{9}{40}Pr^2\alpha_3 + \frac{1}{10}Pr\alpha_3 R\lambda^2 sin(\gamma)^2\right)\eta^5 \quad (44)$$

We avoid listing the other components. However according to Eqs. 28(a,b,c), we obtain $f(\eta)$ up to $0(\eta^8)$ and $h(\eta)$ up to $0(\eta^8)$ and $\theta(\eta)$ up to $0(\eta^7)$ as follows:

$$f(\eta) = \eta + \frac{1}{2}\alpha_1\eta^2 + \left(-\frac{1}{6}\lambda^2 sin(\gamma)^2 - \frac{1}{6}A\lambda sin(\gamma) + \frac{1}{6}A + \frac{1}{6}\right)\eta^3 + \left(\frac{1}{24}\alpha_1 + \frac{1}{24}\alpha_1 A\right)\eta^4$$
$$+\left(\frac{1}{120}\alpha_1^2 - \frac{1}{120}A^2\lambda sin(\gamma) + \frac{1}{120}A^2 - \frac{1}{120}A\lambda^2 sin(\gamma)^2 + \frac{1}{120}A\right)\eta^5$$
$$+\left(-\frac{1}{360}\alpha_1\lambda^2 sin(\gamma)^2 - \frac{1}{360}\alpha_1 A\lambda sin(\gamma) + \frac{1}{720}\alpha_1 + \frac{1}{720}\alpha_1 A^2 + \frac{1}{360}A\alpha_1\right)\eta^6$$
$$+\left(-\frac{1}{5040}\alpha_1^2 + \frac{1}{2520}\alpha_1^2 A\right)\eta^7 - \frac{1}{40320}\alpha_1^3\eta^8 + \ldots \quad (45)$$

$$h(\eta) = \frac{1}{2}\alpha_2\eta^2 + \frac{1}{6}\alpha\eta^3 + \left(\frac{1}{24}A\alpha_2 - \frac{1}{24}A\right)\eta^4 + \left(\frac{1}{120}\alpha_2\alpha_1 - \frac{1}{120}\alpha + \frac{1}{120}A\alpha\right)\eta^5$$
$$+ \left(\frac{1}{720}A^2\alpha_2 - \frac{1}{360}\alpha_2 A\lambda sin(\gamma) - \frac{1}{360}\alpha_2\lambda^2 sin(\gamma)^2 + \frac{1}{360}\alpha_2 + \frac{1}{360}A - \frac{1}{720}A^2\right)\eta^6$$
$$+ \left(\frac{1}{2520}A\alpha_1 + \frac{1}{2520}A\alpha_2\alpha_1\right)\eta^7 - \frac{1}{40320}\alpha_2\alpha_1^2\eta^8 + \ldots \tag{46}$$

$$\begin{aligned}\theta(\eta) &= 1 + \alpha_3\eta - \frac{1}{2}\frac{Pr\alpha_3}{4R+3}\eta^3 - \frac{1}{8}\frac{Pr\alpha_3\alpha_1}{(4R+3)}\eta^4 + \frac{1}{(4R+3)^2}\\ &\left(\frac{1}{10}Pr\alpha_3 AR\lambda sin(\gamma) - \frac{3}{40}Pr\alpha_3 - \frac{1}{10}Pr\alpha_3 AR + \frac{3}{40}Pr\alpha_3 A\lambda sin(\gamma) - \frac{3}{40}Pr\alpha_3\right.\\ &\left. A + \frac{3}{40}Pr\alpha_3\lambda^2 sin(\gamma)^2 - \frac{1}{10}Pr\alpha_3 R + \frac{9}{40}Pr^2\alpha_3 + \frac{1}{10}Pr\alpha_3 R\lambda^2 sin(\gamma)^2\right)\eta^5\\ &+\frac{1}{(4R+3)^2}\left(-\frac{1}{60}Pr\alpha_3\alpha_1 RA + \frac{1}{8}Pr^2\alpha_3\alpha_1 - \frac{1}{80}Pr\alpha_3\alpha_1 - \frac{1}{60}\right.\\ &\left. Pr\alpha_3\alpha_1 R - \frac{1}{80}Pr\alpha_3\alpha_1 A\right)\eta^6 + \frac{1}{(4R+3)^2}\left(-\frac{1}{560}Pr\alpha_3\alpha_1^2 - \frac{1}{420}\right.\\ &\left. Pr\alpha_3 R\alpha_1^2 + \frac{1}{56}Pr^2\alpha_3\alpha_1^2\right)\eta^7 + \ldots\end{aligned} \tag{47}$$

5. The padé Approximants

It is well known that Padé approximations [29] have the Advantage of manipulating the polynomial approximation into a rational function of polynomials. This manipulation provides us with more information about the mathematical behavior of the solution. Besides that, power series are not useful for large values of η, say $\eta = \infty$. Boyd [30] and others have formally shown that power series in isolation are not useful for handling boundary value problems. Therefore, the combination of the homotopy perturbation method with the Padé approximation provides an effective tool for handling boundary value problems on infinite or semi-infinite domains. It is a known fact that Padé approximation converges on the entire real axis if $f(\eta)$, $h(\eta)$ and $\theta(\eta)$ are free of singularities on the real axis. More importantly, the diagonal approximants are most accurate approximants; therefore we have to construct only diagonal approximants. Using the boundary conditions $f'(\infty) = \lambda sin\gamma$, $h''(\infty) = 0$ and $\theta(\infty) = 0$ the diagonal ap-

proximant [M/M] vanishes if the coefficient of η with the highest power in the numerator vanishes. Choosing the coefficients of the highest power of η equal to zero, we get polynomial equations in α_1, α_2, α_3 which can be solved very easily by using the built in utilities in the most manipulation languages such as Maple and Mathematica.

6. Results and Discussion

System of nonlinear ordinary differential Eqs . (15), (16) and (23) with transformed boundary conditions (17), (21) and (24) for different values of λ, γ, A, R and Pr were obtained using homotopy Perturbation method (HPM) employing Padé technique. Obtained results are shown in Figs. 2-19.

Figs. 2 and 3 show that increasing the number of HPM terms does not affect on the convergence, while HPM– Padé solution can perfectly control it. Figs. 4 and 5 clearly show the correct behavior of velocity and temperature profiles that have been obtained by HPM– Padé in comparison to HPM. The results of HPM– Padé are in good agreement with numerical results, while HPM result is in less accurate predictions. Figs. 6 and 7 present that increasing the order of Padé approximation, simplifies the procedure of obtaining the correct values of velocity and temperature such that, by increasing the value of η_μ from 5 to 8, the velocity and temperature profiles have not been changed for Padé [20, 20] but it is not true for the other orders of Padé. Figs.8 and 9 depict the velocity profiles for different values of Porosity parameter A and velocity parameter λ striking angle γ. The results indicate that they have positive slopes for $\lambda\sin\gamma > 1$, and the curves reduce with a negative slope for $\lambda\sin\gamma < 1$. It is also observed that for a fixed value of η, the velocity at a point decreases with an increase in the Porosity parameter A for $\lambda\sin\gamma < 1$, while the velocity increases in A for $\lambda\sin\gamma > 1$. Fig. 10 show values of $f(\eta)$, $f'(\eta)$ and $f''(\eta)$ for fixed values of λ=2.5, γ=π/3 and A = 0 and the comparison of them with numerical results.

Figs. 11 and 13 show the streamline patterns for various values of λ, γ and A. It is noticed from these figures that the obliqueness of the oncoming flow increases as $\lambda\sin\gamma$ decreases. It is observed from Figs.11 and 12, and Table 6 that variation of the location of the stagnation point of ξs is at the right of the origin x = 0 for $\lambda\sin\gamma < 1$, but this location is on the left hand side of the origin for $\lambda\sin\gamma > 1$. It can be seen that the slope of the dividing streamline far from the plane becomes steeper as A increases for $\lambda\sin\gamma > 1$, while opposite behavior is observed as A

decreases. Also, It can be seen that the stagnation point is distance from the origin $(x = 0)$ increases as A increases. On the other hand, the simulated streamline are shown in Figs. 13. An excellent match is found between simulation results and HPM- Pad solution.

Figs. 14, 15 and 16 show temperature profiles for several values of λ, γ and Pr, R. It is observed temperature profiles decreases with an increase in λ, γ and Pr and the thermal boundary layer thickness becomes smaller. While the temperature increases with an increase in R.

7. CONCLUSIONS

In this paper we have considered the steady two-dimensional non-orthogonal flow near the stagnation point on a stretching sheet embedded in a porous medium in the presence of radiation effects. The transformed ordinary differential equations has been solved analytically by homotopy perturbation method (HPM) employing Padé technique to exhibit the effects of the stretching parameter λ, striking angle γ, porosity parameter A, radiation parameter R, Prandtl number Pr on the fluid flow and heat transfer characteristics. Obtained series solution is combined with the diagonal Padé approximants to handle the boundary condition at infinity. The excellent agreement of the HPM solutions by numerical methods shows the reliability and the efficiency of the method. This new method accelerated the convergence to the solutions. The HPM combined with the Padé approximant provide a powerful tool to handle physical problems with infinite boundary conditions.

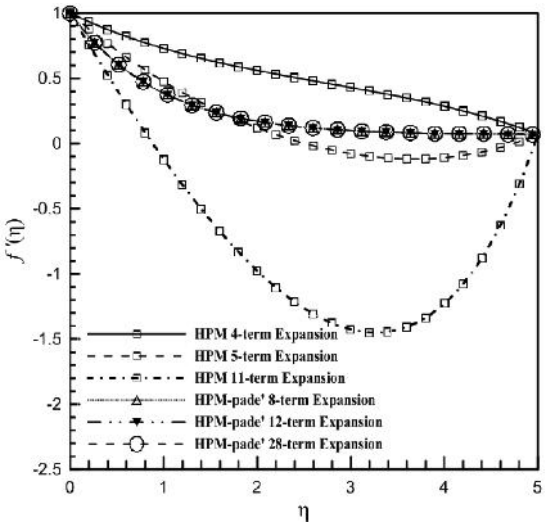

Fig. 2. The effect of increasing the number of HPM and HPM-Padé terms on velocity profile when $\lambda = .1$, $\gamma = \pi/4$ and $A = 0$

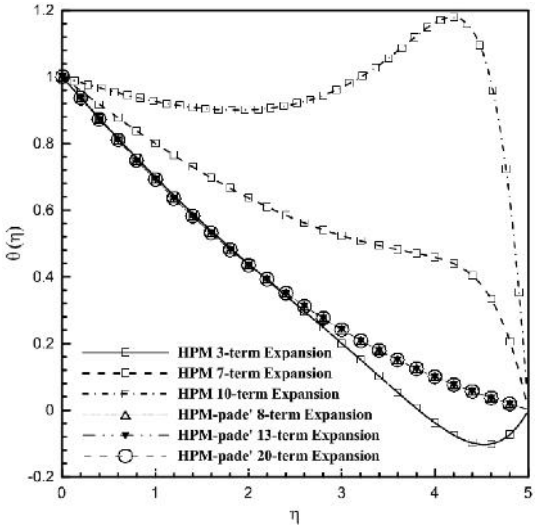

Fig. 3. The effect of increasing the of HPM and HPM-Padé terms on temperature profile when $A = 0$, $R = 1$, $Pr = .71$ and $\lambda = .1$, $\gamma = \pi/3$

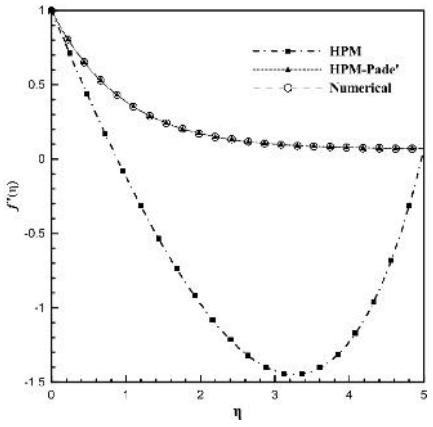

Fig. 4. Comparison of HPM-Padé terms and HPM with numerical solution when $\lambda = .1$, $\gamma = \pi/4$ and $A = 0$

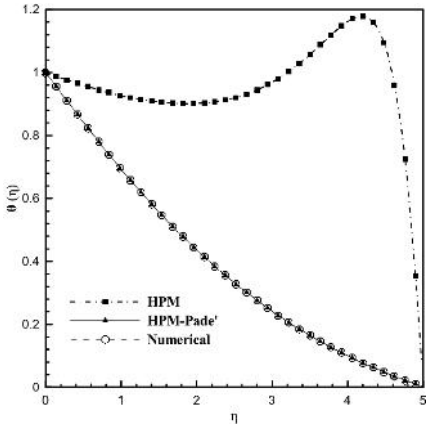

Fig. 5. Comparison of HPM-Padé terms and HPM with numerical solution when $\lambda = .1$, $\gamma = \pi/3$, $R = 1$, $Pr = .71$ and $A = 0$

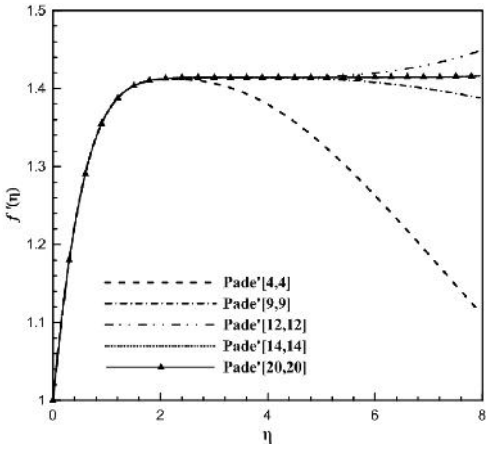

Fig. 6. The effect of increasing the order of HPM-Padé approximation on velocity profile when $\lambda = 2$, $\gamma = \pi/4$ and $A = 0$

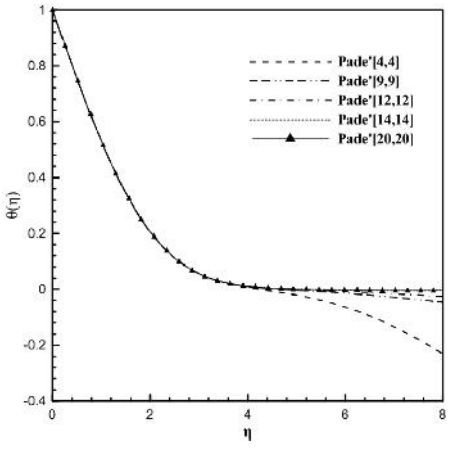

Fig. 7. The effect of increasing the order of HPM-Padé approximation on temperature profile when $\lambda = 2$, $\gamma = \pi/4$, $Pr = 1$, $R = 1$ and $A = 0$

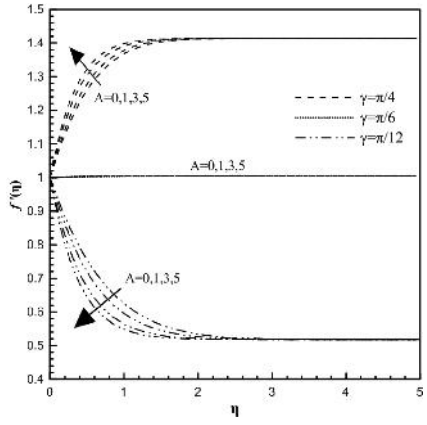

Fig. 8. HPM-Padé solution of $f'(\eta)$ for $\lambda = 2$ and various values of γ and A

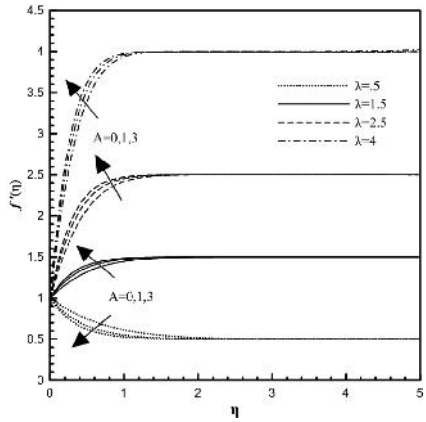

Fig. 9. HPM-Padé solution of $f'(\eta)$ for $\gamma = \pi/2$ and various values of λ and A

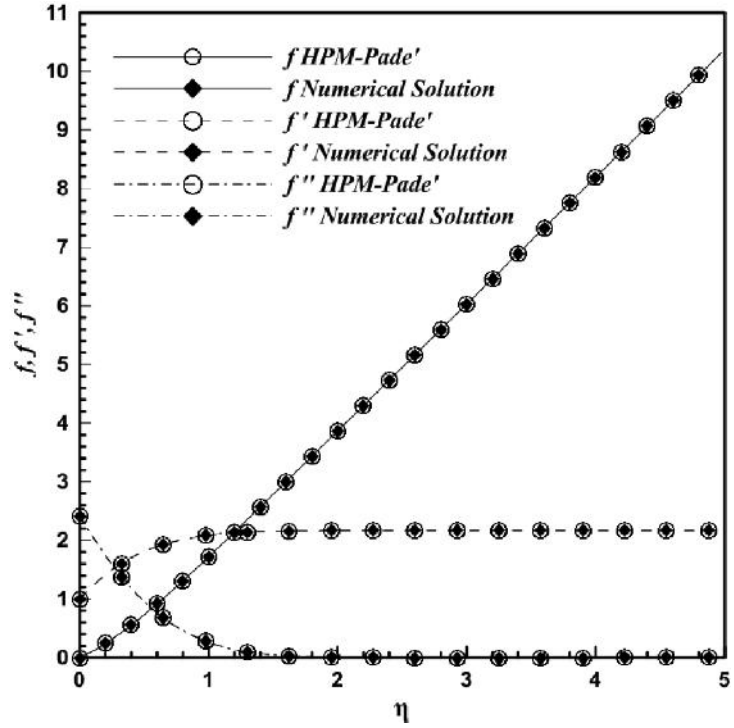

Fig. 10. Comparison of HPM-Padé solution with numerical solution when $\lambda = 2.5$, $\gamma = \pi/3$ and $A = 0$

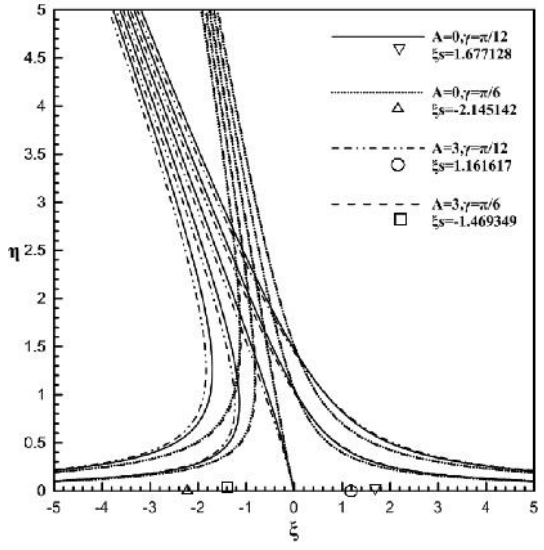

Fig. 11. HPM-Padé solution of streamlines for $\lambda = 2.5$ and various values of γ and A

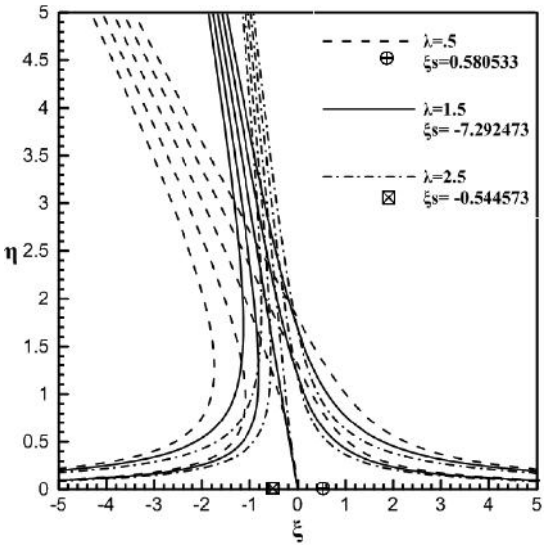

Fig. 12. HPM-Padé solution of streamlines for $\gamma = \pi/4$, $A = 0$ and various λ

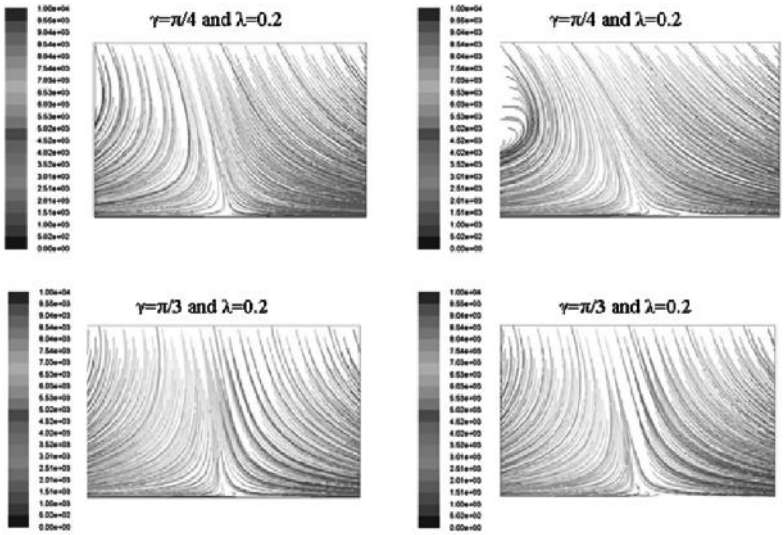

Fig. 13. Numerical simulation of streamlines

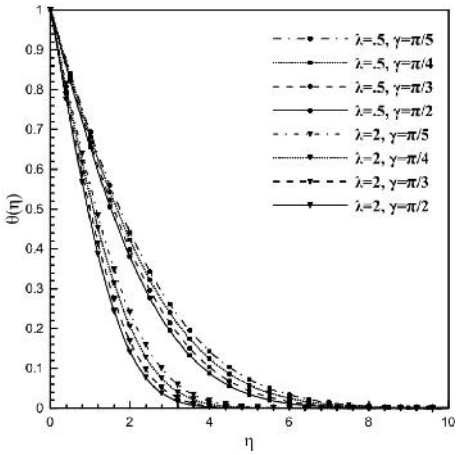

Fig. 14. Temperature profiles for Pr = .71, R = 1, A = 0 and various values of λ and γ

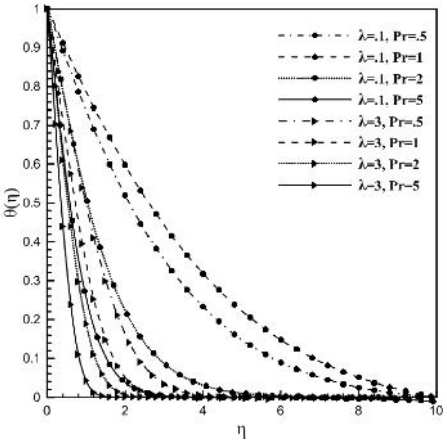

Fig. 15. Temperature profiles for γ = π/3, R = 1, A = 0 and various values of λ and Pr

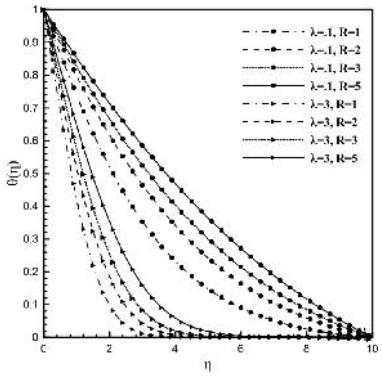

Fig. 16. Temperature profile for γ = π/3, Pr = .71, A = 0 various values of λ and R

REFERENCES

1. P. Weidman and J. Paullet, Analysis of stagnation point flow toward a stretching sheet, *Inter. J. Non-Linear Mechanics*, **42** (2007), 1084-1091.

2. Hiemenz and K. Die, Grenzschicht an einem in den gleichformingen Flussigkeitsstrom eingetauchten graden Kreiszylinder, *Dinglers Polytech. J.*, **236** (1911), 321-324.

3. T. C. Chiam, Stagnation-point flow towards a stretching plate, *J. Physical Soc. of Japan*, **63**(6) (1994), 2443-2444.

4. L. J. Crane, Flow past a stretching plate, *J. Appl. Math. Phys. (ZAMP)*, **21** (1970), 645-647.

5. P. D. McCormak and L. J. Crane, *Physical Fluid Dynamics*, Academic Press, New York, (1973).

6. A. S. Gupta and T. R. Mahapatra, Stagnation-Point Flow Towards a Stretching Surface, *The Can. J. Chem. Engng.*, **81**(2) (2003), 258-263.

7. N. A. Yacob, A. Ishak and I. Pop, Melting heat transfer in boundary layer stagnation-point flow towards a stretching/shrinking sheet in a micropolar fluid, *Computers & Fluids*, **47**(1)(2011), 16-21.

8. M. Z. Salleh, R. Nazar and I. Pop, Forced Convection Boundary Layer Flow at a Forward Stagnation Point with Newtonian Heating, *Chem. Engng. Commun.*, **196**(9) (2009), 987-996.

9. A. Noghrehabadi, R. Pourrajab and M. Ghalambaz, Effect of partial slip boundary condition on the flow and heat transfer of nanofluids past stretching sheet prescribed constant wall temperature, *Inter. J. Thermal Sci.*, **54** (2012), 253-261.

10. D. Li, F. Labropulu and I. Pop, Oblique stagnation-point flow of a viscoelastic fluid with heat transfer, *Inter. J. Non-Linear Mechanics*, **44** (2009), 1024-1030.

11. S. P. Anjali Devi and B. Ganga, Dissipation effects on MHD nonlinear flow and heat transfer past a porous surface with prescribed heat flux, *J. Appl. Fluid Mechanics*, **3** (2008), 1-6.

12. P. R. Sharma and G. Singh, Effects of variable thermal conductivity and heat source/sink on MHD flow near a stagnation point on a linearly stretching sheet, *J. Appl. Fluid Mechanics*, **2** (2009), 13-21.

13. R. Tamizharasi and V. Kumaran, Pressure in MHD/Brinkman flow past a stretching sheet, *Commun. Nonlinear Sci. and Num. Simulation*, **16**(12) (2011), 4671-4681.

14. D. Pal and H. Mondal, Effect of variable viscosity on MHD non-Darcy mixed convective heat transfer over a stretching sheet embedded in a porous medium with non-uniform heat source/sink, *Commun. Nonlinear Sci. Numer. Simulat.*, **15** (2010), 1553-1564.

15. T. Hayat, T. Javed and Z. Abbas, MHD flow of a micropolar fluid near a stagnation point towards a non-linear stretching surface, *Nonlinear Analysis: Real World Applications*, **10** (2009), 1514-1526.

16. J. B. McLeod and K. R. R., On the uniqueness of flow of a Navier–Stokes fluid due to a stretching boundary, *Arch. Ration. Mech. Anal.*, **98** (1987), 358-393.

17. S. J. Liao, *The proposed homotopy analysis technique for the solution of nonlinear problems*, Ph.D., Shanghai Jiao Tong University, (1992).

18. S. J. Liao, *Beyond perturbation: introduction to the homotopy analysis method*, Chapman &Hall/CRC Press (2003).

19. J. H. He, Homotopy perturbation method: a new nonlinear analytical technique, *Appl. Math. Comput.*, **135** (2003), 73-79.

20. J. H. He, A coupling method of a homotopy technique and a perturbation technique for non-linear problems, *Inter. J. Non-Linear Mechanics*, **35** (2000), 37-43.

21. J. H. He, A simple perturbation approach to Blasius equation, *Appl. Math. Comput.*, **140** (2003), 217-22.

22. M. Esmaeilpour and D. D. Ganji, Application of He's homotopy perturbation method to boundary layer flow and convection heat transfer over a flat plate, *Phys. Lett. A*, **372** (2007), 33-8.

23. A. Yildirim, Application of He's homotopy perturbation method for solving the Cauchy reaction–diffusion problem, *Comput. Math. Appl.*, **57**(4) (2009), 612-618.

24. A. Yildirim and H. Koçak, Homotopy perturbation method for solving the space-time fractional advection-dispersion equation, *Adv. Water Resour.*, **32**(12) (2009), 1711-1716.

25. M. Omidvar, A. Barari, M. Momeni and D. D. Ganji, New class of solutions for water infiltration problems in unsaturated soils, *Geomech Geoeng: Int. J.*, **5** (2010), 127-35.

26. D. D. Ganji, The application of He's homotopy perturbation method to nonlinear equations arising in heat transfer, *Phys. Lett. A*, **355** (2006), 337-341.

27. Y. Y. Lok, N. Amin and I. Pop, Non-orthogonal stagnation point flow towards a stretching sheet, *Inter. J. Non-Linear Mechanics*, **41** (2006), 622-627.

28. P. Singh, N. S. Tomer and D. Sinha, Oblique Stagnation-Point Darcy Flow towards a Stretching Sheet, *J. Appl. Fluid Mechanics*, **5**(3)(2012), 29-37.

29. G. A. Baker, *Essentials of Padé Approximants*, Academic Press, London, (1975).

30. J. Boyd, Padé approximant algorithm for solving nonlinear ordinary differential equation boundary value problems on an unbounded domain, *Comput. Phys*., **11**(3) (1997), 299-303.